

# Reinforcement learning-driven de-novo design of anticancer compounds conditioned on biomolecular profiles

Jannis Born\* and Matteo Manica\* and Ali Oskooei\* and María Rodríguez Martínez

IBM Research

4 Säumerstrasse

Rüschlikon, Switzerland 8803

\*Equal contributions

## Abstract

With the advent of deep generative models in computational chemistry, in silico anticancer drug design has undergone an unprecedented transformation. While state-of-the-art deep learning approaches have shown potential in generating compounds with desired chemical properties, they entirely overlook the genetic profile and properties of the target disease. In the case of cancer, this is problematic since cancer is a highly genetic disease in which the biomolecular profile of target cells determines the response to anticancer therapy. Here, we introduce the first deep generative model capable of generating anticancer compounds given a specific target biomolecular profile. Using a reinforcement learning framework, the transcriptomic profile of cancer cells is used as a context in which anticancer molecules are generated and optimized to obtain effective anticancer compounds for the given context (i.e., transcriptomic profile). Our molecule generator combines two separately pretrained variational autoencoders (VAEs) and a multimodal efficacy predictor – the first VAE generates transcriptomic profiles while the second conditional VAE generates novel molecular structures conditioned on the given transcriptomic profile. The efficacy predictor is used to optimize the generated molecules through a reward determined by the predicted IC50 drug sensitivity for the generated molecule and the target profile. We demonstrate how the molecule generation can be biased towards compounds with high predicted inhibitory effect against individual cell lines or specific cancer sites. We verify our approach by investigating candidate drugs generated against specific cancer types and investigate their structural similarity to existing compounds with known efficacy against these cancer types. We envision our approach to transform in silico anticancer drug design by increasing success rates in lead compound discovery via leveraging the biomolecular characteristics of the disease.

## Introduction

The last two decades have seen a decline in the productivity of the new drug discovery pipelines while the investment into new drug discovery has risen significantly in the same period (Arun 2009). Indeed, only a minimal portion of drug candidates obtain market approval (less than 0.01%), with an estimated 10-15 years until market release and costs that range between one (Scannell et al. 2012) to three billion dollars per drug (Schneider 2019). This low efficiency has been attributed to the high dropout rate of candidate molecules in the early stages of the pipeline, highlighting the need for

more accurate in silico and in vitro models for producing more successful candidate drugs.

In recent years, deep learning methods have gained popularity within the computational chemistry community for helping bridge the innovation gap and improving the efficiency of drug discovery (Chen et al. 2018). Most recently, a number of works have demonstrated the feasibility of in silico design of novel candidate compounds with desired chemical properties (Popova, Isayev, and Tropsha 2018; Gomez-Bombarelli et al. 2018) and established the first benchmarks for in silico drug design (Brown et al. 2018). In all of these models, the generative process is controlled via a structurally driven evaluator (or critic) that biases the generation of a chemical to satisfy the required chemical structural properties. While very effective in generating compounds with desired chemical properties, these methods fail to integrate information about the cellular environment in which the drug is intended to act. As such, these solutions require wet-lab validation experiments to assess whether the drug is effective for the disease of interest. In addition to the initial validations, the discovery pipeline involves a long sequential process that builds upon high-throughput screenings, ADMET-assessments (absorption, distribution, metabolism, excretion and toxicity, i.e., criteria for the pharmacological activity of a compound) and a lengthy phase of clinical trials.

The costs of the experimental and clinical phase, in terms of time and resources, can be prohibitive and any solution that helps to reduce the number of required experimental assays can provide a competitive advantage and reduce time to market. To this end, we present a deep reinforcement learning based model for anticancer molecule generation that builds on top of the previous approaches and for the first time, enables generation of novel anticancer compounds while taking into account the disease context encoded in the form of gene expression profile of the disease e.g., tumor. In our approach, the evaluation mechanism used to fine-tune the generator, does not only depend on a proposed candidate compound but also on the genetic profile of the target cell, disease or patient. In other words, our generator designs candidate compounds that are tailored individually to patient-specific disease profiles and incorporate the information from the target environment for the drug (e.g, tissue, tumor type), with the goal of increasing the efficacy of the designed candidates. The two main components of our framework are described in more

detail below:

**Conditional Generator ( $\mathcal{G}$ )** A molecule generator that produces a candidate molecular structure represented by the SMILES string representation of the molecule. SMILES are applied extensively in QSAR and predictive deep learning models and have been recently shown to be superior to (functional) fingerprint-based (e.g., ECFP) generative models for molecules (Bjerrum and Sattarov 2018; Oskooei et al. 2018a). The generative process is conditioned on a target biomolecular profile e.g., from a patient or a disease. The generator can optionally be primed with an arbitrary compound or molecular substructure, e.g., an approved drug with known inhibitory effects against the biomolecular profile of interest or a functional group. Such a generator can be implemented using any generative model for sequence or text generation, including sequence-to-sequence models like the transformer for neural machine translation (Vaswani et al. 2017), stack-augmented recurrent neural networks (RNN, (Joulin and Mikolov 2015)), generative adversarial networks (GANs, (Goodfellow et al. 2014)), variational autoencoders (VAE, (Kingma and Welling 2013)), a combination of the latter two (Rosca et al. 2017) or adversarial autoencoders (AAE, (Makhzani et al. 2015)). Our approach is inspired by (Gomez-Bombarelli et al. 2018), who used a VAE with convolutional units in the encoder to learn a structurally ordered, smooth latent space of molecular structures using a dataset of 250k training molecules. The authors demonstrate how the latent space can be trained to encode functional instead of structural similarity through joint training of a property predictor. In a similar work, (Kang and Cho 2018) went one step further and developed a VAE-based model that jointly performs property prediction and molecule design conditioned on that chemical property. Our proposed generator in this work, combines two VAEs one for generating biomolecular profiles and a second VAE, based on stack-augmented GRUs, for generating molecular structures conditioned on the biomolecular profile generated by the first VAE.

**Critic ( $\mathcal{C}$ )** A predictive model that evaluates the efficacy of the generated compound on the target profile. The critic module ingests the chemical structure of the generated compound as well as the target biomolecular profile and returns a reward that is a strictly decreasing function of the predicted IC50 drug sensitivity for the given compound-profile pair. The reward returned by the critic for a generated compound is then used, in a reinforcement learning (RL) framework, to update the generator model and improve the efficacy of the generated molecule for the given profile. The critic is trained independently using the drug screening data from the GDSC (Yang et al. 2012) and CCLE (Barretina et al. 2012) databases.

The training procedure for the generator and critic models consists of two stages. In the first stage, each model is trained independently and in the second stage, the generative model is retrained and optimized via a reinforcement

learning approach with a reward coming from the critic module, as previously described. The goal of RL optimization is to fine-tune the generative model such that it generates (novel) compounds that have maximal efficacy against a given biomolecular profile.

In this work, we emphasize profile-specific compound generation and only optimize the generator using a single critic for IC50 drug sensitivity but it is noteworthy, that besides the inhibitory efficacy, there is a myriad of chemical properties that crucially influence the potential of a candidate molecule for becoming an anticancer compound. It hence may be beneficial to train the generator with a panel of critic modules, for example penalizing general cytotoxicity (Yang et al. 2018), boost druglikeness (QED, (Bickerton et al. 2012)), synthetic accessibility scores (SAS, (Ertl and Schuffenhauer 2009)), solubility (Savjani, Gajjar, and Savjani 2012) and bioavailability or evaluate syntactic validity of the generated SMILES strings.

## Methods

As Figure 1 showcases, the end-to-end architecture of our proposed model consists of two main components: the conditional generator and the critic. In this section, we describe each component and the associated theory in detail.

### Conditional generator

The conditional generator (Figure 1C) consists of two VAEs that are fused together: 1) a denoising VAE (D-VAE, Figure 1A) for cancer profile generation (i.e., profile VAE, PVAE) and 2) a sequential VAE (SVAE) for SMILES sequence generation (see Figure 1B).

The variational autoencoder is a generative model that is the marriage of a directed graphical model and an autoencoder. Given an observed variable  $x$ , the VAE assumes that  $x$  is generated from an unobserved latent variable  $z$  and aims to model the data distribution,  $p(x)$ . In summary,  $z$  is generated from the prior distribution,  $p_\theta(z)$  and  $x$  is generated from the generative distribution,  $p_\theta(x|z)$ , estimated by a deep neural network. The main challenge here is the posterior inference due to its intractability. VAE addresses this challenge by approximating the posterior with a tractable distribution  $q_\phi(z|x)$  which is assumed to be a Gaussian with diagonal covariance,  $\mathcal{N}(\mu, \text{diag}(\sigma^2))$ . Combining the variational distribution as the encoder and the generative distribution as the decoder and in combination with reparameterization of  $z$ , VAE builds an end-to-end neural network that can be trained via backpropagation with the objective of maximizing the variational lower bound and in turn the data likelihood. The detailed derivation and equations for the variational autoencoder can be found elsewhere (Kingma and Welling 2013; Sohn, Lee, and Yan 2015; Pagnoni, Liu, and Li 2018).

SVAE and PVAE are initially pretrained in isolation. SVAE is trained on bioactive drug-like molecules to learn the syntax of valid SMILES and general molecular semantics. PVAE is trained on gene expression profiles to learn a consistent latent representation for biomolecular signatures. Following the initial pretraining step, the encoder of the PVAE is fused with the decoder of the SVAE via their latent space. The

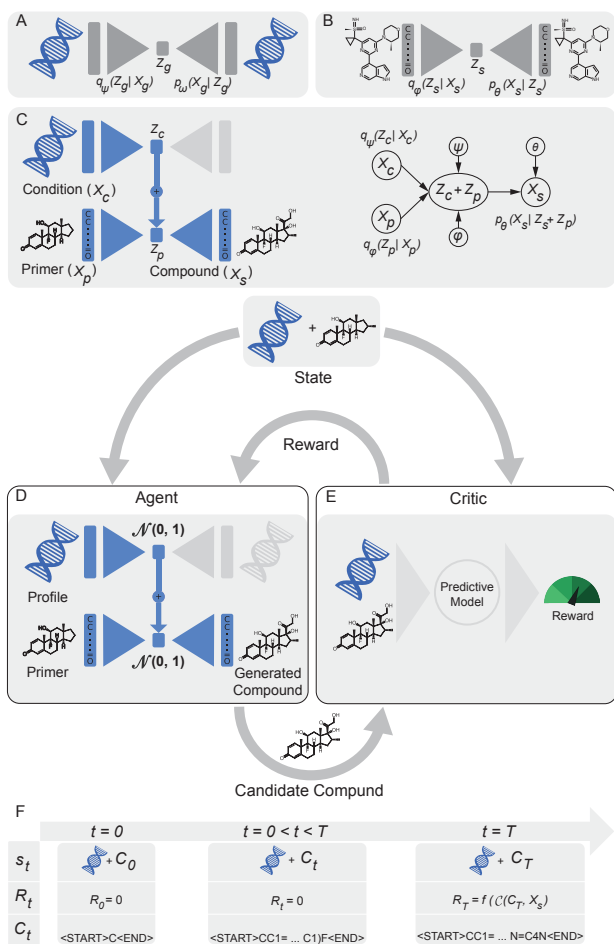


**Figure 1: The schematic illustration of the proposed framework for anticancer compound design against specific cancer profiles.** A biomolecular profile VAE (PVAE) shown in (A) and a sequential compound generator VAE (SVAE) shown in (B) are combined to obtain a conditional molecule generator depicted in (C). Each of the PVAE, SVAE and the predictive critic are pretrained independently. The conditional generation process starts with a biomolecular profile of interest e.g., transcriptomic profile from an individual patient. The given profile is encoded into the latent space of gene expression profiles and is then decoded as shown in (C) to produce a candidate compound. The generative process can be “primed” through encoding a known, effective compound or a functional group with the molecular encoder. The generated candidate compound is then evaluated against the target profile of interest through a drug sensitivity prediction model or the critic (E). The reinforcement learning based optimization is conducted by maximizing the reward given by the critic. Over the course of training, the generator will thus learn to produce candidate compounds with higher and higher efficacy. The RL training evolution including the state ( $s_t$ ), the reward ( $R_t$ ) and the candidate compound ( $C_t$ ) during a complete training cycle are shown in (E).  $\langle \text{START} \rangle$  is the start and  $\langle \text{END} \rangle$  is the end token.

combination of the two models enables us to learn a latent space that links biomolecular profiles and chemical structures providing an effective way to sample novel compounds given a particular gene expression profile. In the final training phase, the weights of the fused model are fine-tuned using a reward given by the critic in a reinforcement learning framework. The components of the conditional generator namely PVAE and SVAE are described in more detail below.

**PVAE** As a model for generation of novel transcriptomic profiles, a D-VAE is trained on gene expression profiles from healthy and cancerous human tissues (as measured by RNA-Seq samples). The gene expression data was subsampled to 2,128 most informative genes for drug sensitivity in cancer following the network propagation procedure described in (Oskooei et al. 2018b). The D-VAE learns meaningful, lower-dimensional encodings of biomolecular cancer cell profiles. These encodings are later used by the conditional generator to generate anticancer compounds that are effective for treating cancer cells with the given profile. By learning the data distribution, PVAE is able to generate an unlimited number of transcriptomic profiles and thereby serves to address the problem of data scarcity which is a common obstacle in using deep learning approaches with omic data.

**SVAE** Both the encoder and the decoder of SVAE consisted of a set of bidirectional, stack-augmented gated recurrent units (GRU) shown in Figure 2A. The SMILES language is a context-free language according to the Chomsky hierarchy (Chomsky 1956) and requires a balanced set of parentheses which poses an additional syntactical challenge compared to natural language processing models. As such, network architectures that process SMILES sequences must have the ability to keep track of and, in essence, count the ring opening and closing symbols (parentheses) in a molecule. This capability necessitates use of stack memory (Hopcroft and Ullman 1969) and was demonstrated to be lacking in standard RNNs such as LSTMs, particularly for processing long sequences (Joulin and Mikolov 2015). To enable counting, (Joulin and Mikolov 2015) introduced stack-augmented RNN units which can learn to count by complementing RNNs with a differentiable push-down stack operated through learnable controllers,  $op_t$  at step  $t$ , that involve three operations: PUSH, POP and NO-OP.

$$op_t = \mathbf{s}(W_{op}h_t), \quad (1)$$

where  $h_t$  is the hidden state,  $W_{op}$  is a  $3 \times H$  matrix ( $H$  being the dimension of hidden state) and  $\mathbf{s}$  is the softmax function. At each time step the controller probabilities are determined from Equation 1 and the stack memory is updated using the learned controller via a multiplicative gating mechanism:

$$\begin{cases} S_t[0] &= op_t[\text{PUSH}]\mathbf{s}(W_{so}h_t) + op_t[\text{POP}]S_{t-1}[1] + \\ & op_t[\text{NO-OP}]S_{t-1}[0] \\ h_t &= \mathbf{s}(W_iX_t + W_Rh_{t-1} + W_{si}S_{t-1}) \end{cases} \quad (2)$$

where  $S_t$  is the stack,  $W_{so}$  is a  $1 \times H$  matrix and  $W_{si}$  is a  $H \times N$  matrix ( $N$  being the stack height).  $W_i$  is the input matrix applied to the sequence and  $W_R$  is the recurrent matrix.

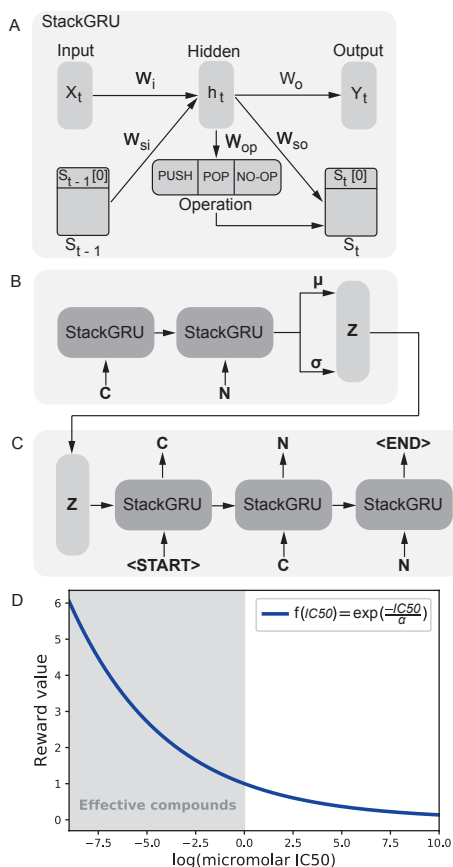


**Figure 2: The StackGRU and SVAE architecture and the adopted reward function.** A) The stack-augmented GRU (StackGRU) architecture employed in our generator with three possible operations at each time-step: PUSH, POP and NO-OP. The operation vector is determined through a softmax from the hidden state of each time step and as such each operation is a real number between 0 and 1 and all actions sum up to 1. B) The schematic illustration of the SVAE consisting of StackGRU units that encode the SMILES sequences into multivariate Gaussians with parameters of  $\mu$  and  $\sigma$ . C) The decoder StackGRU units that reconstruct the SMILES sequence from a latent representation,  $Z$ , sampled from the multivariate Gaussian. D) The reward function  $f(IC_{50})$  was used to map the  $IC_{50}$  value predicted by the critic to a reward that was subject to maximization in our adopted RL framework. To produce the plot,  $\alpha$  was set to 5 and 6 respectively.

It should be noted that for the sake of brevity, we only show the update equation for the topmost element of the stack in Equation 2. The detailed equations for the stack augmented RNNs can be found elsewhere (Joulin and Mikolov 2015).

## Critic

The critic is a multimodal drug sensitivity prediction model which evaluates the efficacy of any given candidate compound against a given biomolecular profile (e.g., gene ex-

pression of a cancer cell line) and returns a real-valued non-negative reward. More specifically, The critic receives a compound-profile pair consisting of the candidate compound represented by its SMILES string and the target transcriptomic profile and returns a positive reward which is a function of the predicted  $IC_{50}$  of the candidate compound for the target profile. The details of the reward function are discussed in the following section. The architecture implemented for the critic is based on multiscale convolutional encoders as proposed in (Manica et al. 2019).

## The RL framework

As briefly mentioned earlier, the conditional generator is re-trained in combination with the critic in a reinforcement learning-based optimization process that fine-tunes the generative model for generation of molecules that target the given gene expression profile (GEP). As a first step, the target GEP is encoded into its latent space,  $Z_c$ , as shown in Figure 1C. The resulting representation is then added to the latent encoding of a primer compound or substructure,  $Z_p$ . This additive latent representation is similar in concept to the conditional VAE with additive Gaussian encoding space (AG-CVAE) introduced by (Wang, Schwing, and Lazebnik 2017). The main difference is that in their model the additive latent space is encoded in a variational inference framework while we re-train and optimize the additive encoding in a RL reward maximization framework. It is noteworthy, that using a primer compound or substructure is optional and if no priming compound is used, simply the latent space representation of the <START> token is added to the latent encoding of the target GEP. The advantage of using a primer is that it enables injection of prior knowledge into the model by starting the generative process from an existing and proven effective compound or functional group – instead of designing a compound from scratch. Next, the conditional generator decodes the latent encoding,  $Z_c + Z_p$ , and generates a molecular structure that, in combination with the GEP, is fed to the critic to produce a certain reward for the generated compound, as illustrated in Figure 1D and E. Once the reward is determined, it is used in a RL framework inspired by (Popova, Isayev, and Tropsha 2018), to update the parameters of the conditional generator consisting of the two encoders (i.e.,  $\psi$  and  $\varphi$ ) and the decoder (i.e.,  $\theta$ ).

The framework consists of the conditional generator,  $\mathcal{G}$ , as the *agent* and the  $IC_{50}$  prediction model,  $\mathcal{C}$ , as the *critic*.  $\mathcal{G}$  is parametrized through  $\Theta = \{\psi, \varphi, \theta\}$ , i.e., the weights of two pretrained encoders and the decoder as shown in Figure 1C, while  $\mathcal{C}$  is a pretrained drug sensitivity prediction model with fixed weights. We aim to optimize the  $\Theta$  parameters of  $\mathcal{G}$  to produce candidate compounds,  $C_T$ , that target a specific GEP,  $X_c$ , by means of a reward given by  $\mathcal{C}$ ,  $R_T$ , based on the  $IC_{50}$  value estimated for the pair  $C_T$  and  $X_c$ .

The set of possible actions  $a$  that  $\mathcal{G}$  can take is a set  $\mathcal{A}$ , that is a vocabulary of all characters and symbols that comprise all common canonical SMILES (i.e., the vocabulary of the SMILES language). The set of states  $\mathcal{S}$  is defined as all possible SMILES strings, with a length between 0 and  $T$  characters, and the profile of interest. Molecule generation is a sequential process where  $\mathcal{G}$  samples an action  $a_t$

at each time step  $0 < t < T$  from its generative probability distribution  $p(a_t|s_{t-1})$  resulting in a candidate compound,  $C_t$ , at each time step as described in Figure 1F, where  $s_{t-1} = s_{t-1}(C_{t-1}, X_c)$ . The terminal states are a subset of all states,  $s_T \in S^* \subset S$ , that are reached when either  $t = T$  or when the terminal action  $a_T = \langle \text{END} \rangle$  (the end token) has been produced.

The task of  $\mathcal{G}$  is to utilize its parameters  $\Theta$  to learn a policy  $\Pi(\Theta)$  such that:

$$\Pi(\Theta) = \sum_{s_T \in S^*} p_{\Theta}(s_T) R(s_T) \quad (3)$$

is maximized, where the reward is the output of the critic scaled by a reward function  $f$  that we will introduce shortly  $R_T = R(s_T) = f(\mathcal{C}(C_T, X_c))$ . In other words, the parameters of  $\mathcal{G}$ ,  $\Theta$ , are re-trained and optimized such that, given a particular cell profile  $X_c$ , the probability  $p_{\Theta}$  to generate a SMILES string,  $C_T$ , that receives a maximal reward,  $R_T$ , from the critic  $\mathcal{C}$  is maximal. It is noteworthy that in our framework, the reward is calculated only for the terminal states,  $S^*$ , as previously defined. In other words, all intermediate rewards  $R(s_t) = 0$  where  $t < T$ . As the sum is intractable to be computed exactly, it is approximated through sampling terminal states  $s_T$  on which the gradient can be computed using the REINFORCE algorithm (Williams 1992). Figure 2D presents the reward function,  $f$ , that was adopted for determining the reward from the IC50 prediction,  $\mathcal{C}(s_T)$ , given by the critic.

The reward function,  $f(IC50)$ , is computed as follows:

$$f(IC50) = \exp\left(\frac{-IC50}{\alpha}\right) \quad \text{where } \alpha \in \mathbb{R}^+ \quad (4)$$

In this function,  $\alpha$  is a tunable hyperparameter that determines how much the generator is rewarded for designing effective versus ineffective compounds, i.e., a smaller  $\alpha$  leads to a greedier generator.

## Data and implementation

### Chemical structure

We used the SMILES representations of compounds included in the ChEMBL (Bento et al. 2013) database. ChEMBL is a database of bioactive drug-like small molecules which contains SMILES representation of 1,879,206 molecules. The data in ChEMBL is curated from the primary scientific literature, and cover a significant portion of the SAR and discovery of modern drugs (Bento et al. 2013). In this work we pretrained the SVAE on 1,576,904 molecules from ChEMBL, a database of bioactive molecules with drug-like properties (Gaulton et al. 2016). 10% of the molecules were held out for performance validation.

### Gene expression

In order to train the PVAE, we employed a dataset consisting of 11,592 RNA-Seq gene expression profiles from healthy and cancerous human human tissue from the TCGA database and validated on 1,289 samples from the same database (Weinstein et al. 2013). The number of genes was

reduced to 2,128 genes following a network propagation over the STRING (Szklarczyk et al. 2014) PPI network to extract the most relevant genes to cancer. For RL optimization of the  $\mathcal{G}$ , we made use of the gene expression profiles publicly available as part of the Genomics of Drug Sensitivity in Cancer (GDSC) (Yang et al. 2012) and the Broad Institute Cancer Cell Line Encyclopedia (CCLE) (Barretina et al. 2012) databases. These databases contain genomic and transcriptomic profiles of ~1000 cancer cell lines. We based our models on gene expression data as it has been shown to be more predictive of drug sensitivity in comparison to genomics (i.e., copy number variation and mutations) or epigenomics (i.e., methylation) data (Oskooei et al. 2018b; Menden 2016).

### Drug sensitivity

Drug sensitivity data (i.e., IC50) from the GDSC (Yang et al. 2012) and CCLE (Barretina et al. 2012) databases were used to train the IC50 prediction model or the critic ( $\mathcal{C}$ ). These datasets contain screening results of more than a thousand genetically profiled human pan-cancer cell lines with a wide range of anti-cancer compounds (265 compounds for GDSC and 531 compounds for CCLE, as of the writing of this paper). The screened compounds include chemotherapeutic drugs as well as targeted therapeutics from various sources. We used the screening data for targeted small molecules to train the IC50 prediction model.

### Implementation and training details

All models were implemented in PyTorch 1.0 and trained on a cluster equipped with POWER8 processors and a NVIDIA Tesla P100.

**PVAE** The model consisted of four dense layers of [1024, 512, 256 and 200] neurons with ReLU activation function and dropout of  $p = 0.2$  in both, the encoder and the decoder. The dimensionality of the latent space ( $n$ ) was set to 128. We minimized the variational loss, consisting of the reconstruction loss and KL divergence, using Adam optimizer ( $\beta_1 = 0.9$ ,  $\beta_2 = 0.999$ ,  $\epsilon = 1e-8$ ) and a decreasing learning rate starting at 0.001 (Kingma and Ba 2014). To further regularize the PVAE, denoising methods were employed by 1) employing a dropout of 0.1 on the input genes and 2) adding noise to gene expression values ( $\epsilon \sim \mathcal{N}(0, 0.1)$ ). The model was trained with a batch size of 64 for a maximum of 2000 epochs.

**SVAE** The model was trained on molecules provided in SMILES notation, with the longest molecules consisting of 1423 tokens. Both encoder and decoder consisted of two layers of bidirectional GRU (hidden size of 128, dropout of 0.1 at the first layer), each complemented with 50 parallel memory stacks with the depth of 50. The latent space of SVAE had the same dimensionality as the PVAE (128) to enable the addition of encodings. Similar optimization parameters as PVAE were used. This model further utilized teacher forcing (Williams and Zipser 1989), i.e., the model’s output is conditioned on the previous ground truth sample as opposed to its generated output. Whilst this significantly simplifies learning, it

may drive the generator to predominantly relying on the decoder (thus neglecting the latent encoding), commonly known as the posterior collapse (Pagnoni, Liu, and Li 2018). The problem of posterior collapse was resolved by applying a token dropout rate of 0.1 during teacher forcing as suggested by (Bowman et al. 2015). In addition to token dropout, KL cost-annealing (Bowman et al. 2015) was employed during training. The model was trained with a batch size of 128 for a maximum (early stopping) of  $\sim 110,000$  steps (i.e., exactly 10 epochs) During training, KL cost-annealing as described in (Bowman et al. 2015) was explored in order to trade-off reconstruction and KL loss.

**Critic** The critic was trained using the parameters reported in (Manica et al. 2019) and replicating the best performing architecture based on multiscale convolutional encoders. The model has been trained on a merge of the GDSC and the CCLE datasets.

**RL training** In order to maximize equation 3, we employed Adam optimizer ( $\beta_1 = 0.9$ ,  $\beta_2 = 0.999$ ,  $\varepsilon = 1e-4$ , weight decay  $1e-4$ ) and a decreasing learning rate starting at  $1e-5$ . The gradients were clipped to 2 to prevent  $\mathcal{G}$  from destroying its chemical knowledge about SMILES syntax obtained through pretraining on ChEMBL. For the scaling of the reward function in Equation 4 we set  $\alpha = 5$ .

## Results

### PVAE generation of gene expression profiles

The pretraining results of the PVAE are shown in Figure 3A, B and C. As shown in Figure 3C, the reconstructed samples (blue plot) correctly mimic the distribution of gene expression within the original data (red plot). Furthermore, the sampled GEP follow the same lognormal distribution as the original data. Overall, the results suggest that the pretrained PVAE is able to generate new realistic GEPs of human cells.

### SVAE generation of molecular structures

Figure 3D, E and F provides a quantitative analysis of the SVAE results following pretraining for 10 epochs with  $\sim 1.4$  million structures from the ChEMBL database. Figure 3D demonstrates the evolution of the reconstruction loss and KL divergence during the course of training. As previously mentioned, to tackle posterior collapse, we explored various levels of token dropout for the decoder of SVAE with higher keep probabilities showing more favorable outcomes as demonstrated in Figure 3E. To investigate the novelty and diversity of the generated molecules, we sampled 10,000 molecules by decoding random points from the latent space and utilized a well-established chemical structure similarity, the Tanimoto similarity (i.e., Jaccard Index) to compare the ECFP of a subset of 1000 generated molecules with the training and test data from ChEMBL. Figure 3F presents the distributions of the highest Tanimoto similarity between each generated compound and all compounds in training and test dataset respectively. Only a negligible fraction of the generated molecules existed in either of the datasets, whereas the vast majority had a Tanimoto similarity ( $\tau$ ) between 0.2

and 0.6 suggesting that our model learned to propose novel molecular structures from the chemical space of about  $10^{30}$  to  $10^{60}$  molecules (Polishchuk, Madzhidov, and Varnek 2013). Overall, 96.2% of the 10,000 generated molecules were valid molecular structures (validity assessed via RDKit) surpassing the state of the art results reported by (Popova, Isayev, and Tropsha 2018) using stack-augmented GRUs trained on the ChEMBL database (95% SMILES validity). In addition, the vast majority (99.8%) of our valid generated molecules were unique.

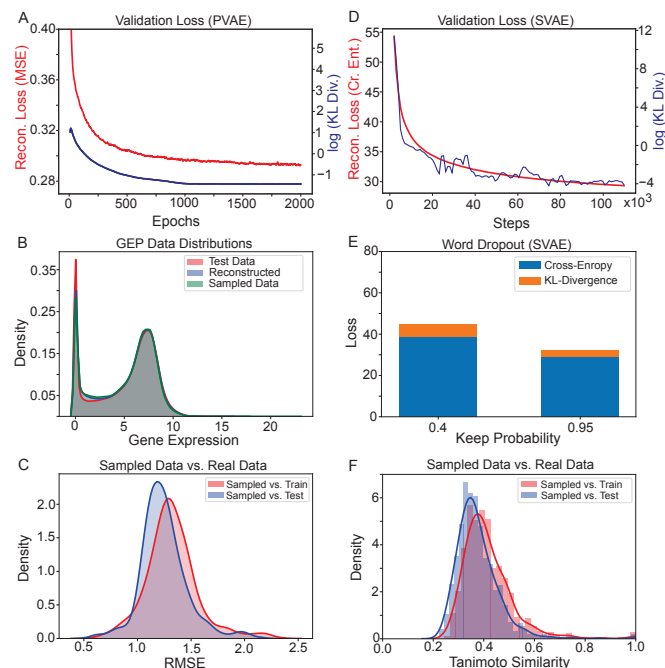


**Figure 3: Results of pretrained PVAE and SVAE models.** A) Development of validation error over the course of training. Reconstruction loss (MSE) and KL divergence are shown separately for comparison. B) Distribution of gene expression values in real, reconstructed and generated samples. C) Sampled (i.e., generated) data from the latent space of PVAE compared against training and test datasets from TCGA demonstrating novelty and diversity of the generated data. D) Development of validation error over the course of training. Reconstruction loss (red, cross-entropy between target and generated SMILES) is shown separately from the KL divergence (shown in log scale for visual clarity). One epoch corresponds to  $\sim 11,000$  training steps. E) The two losses of our baseline model (keep probability 95%) is compared with a model using higher a word dropout of 60% (KL loss is scaled by a factor 200 for visual clarity). Higher word dropout in the decoder increases the encoder loss, i.e., results in storing more information in the latent space. F) The Tanimoto similarity between the Morgan fingerprints (ECFP) of the generated molecules and the structures from ChEMBL train and test datasets is used to verify that the generated compounds are sufficiently different from the training data.

Figure 4A, showcases a panel of 12 generated molecules

for qualitative assessment of the molecular structures. As seen in the Figure the generated molecules generally share drug-like structural features. To inspect the smoothness of the latent space of molecules, we encoded a reference molecule shown at the top of Figure 4B into the latent space and decoded four points in the vicinity of the reference molecule leading to the generation of structurally similar yet different compounds.

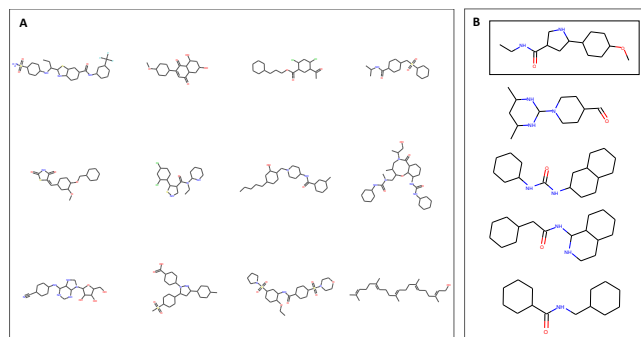


Figure 4: **Qualitative inspection of generated molecules.** A) A sample of 12 molecular structures produced with the SVAE. B) The molecule depicted at the top was encoded into the latent space. The four molecules below show different decodings from the latent space in the vicinity of the starting molecule.

### Disease-specific compound generation

Herein, we present the results of our generator conditioned on gene expression profiles of cancer subtypes. Four different models were trained for four different cancer sites: breast, lung, prostate and neuroblastoma.

For the evaluation of the four models, all generated compounds with an IC<sub>50</sub> value below a concentration of 1  $\mu$ M were considered as *effective*. Moreover, within each cancer site 80% of the cell lines were considered as training cell lines and used to optimize the parameters  $\Theta$  of the conditional generator whereas the remaining 20% were set aside for testing. We used the test cell lines to verify whether the generated compounds have low IC<sub>50</sub> against unseen cell lines of the same cancer site and thereby ensured that the generator indeed considered the profile of interest in generating the compounds.

We observed in the course of RL training, that our model learned gradually to produce compounds with lower (i.e., better) IC<sub>50</sub> values, for the given cancer site, resulting in higher rewards received from the critic. A quantitative and qualitative analysis of the obtained results and proposed candidate compounds is presented in Figure 5.

The first column demonstrates that the IC<sub>50</sub> distribution of candidate compounds proposed by the generative model were successfully shifted towards higher efficacy (i.e., lower IC<sub>50</sub>) through the feedback provided by the critic. In all four cases, a significant portion (between 17% and 30%) of the de-novo designed molecules were assigned a IC<sub>50</sub> value below 1  $\mu$ M, whereas only 1-4% of the candidates generated by the

baseline (i.e., not optimized via RL re-training) model were classified as effective. Although the generation of invalid SMILES structures was not explicitly penalized, the validity rate remained high (87%-94%) compared to the validity rate of the baseline (96%). It is noteworthy that we observed evidence of mode collapse in our model, as a tendency to generate long carbon chains, particularly when the learning rate was set too high or when the temperature parameter of the softmax was too low. The second column of Figure 5 showcases generated molecules that are predicted, by the critic model, as being effective against an unseen cell line from the respective cancer subtype. Overall, as shown in the Figure, our model generated complex molecular structures consisting of a rich set of atoms and common aromatic rings such as e.g., pyrrole which has been associated with anticancer properties (Said Fatahala et al. 2015). As a more realistic case study for drug discovery, in the third column of Figure 5, we showcase novel molecules that were designed specifically for each cancer site, as opposed to a specific cancer cell profile. The cancer site-specific compounds were generated from a single gene expression profile that was characteristic of the respective type of cancer (obtained by averaging all individual cell line profiles). The most effective generated compound for each cancer site is shown here. In all four cancer sites, the shown compound exhibited high predicted efficacy against the average cellular profile of the target site while maintaining efficacy against the majority of individual cell lines for that site. In the last column of Figure 5, we compare the four site-specific candidate compounds with one of their top-3 neighbors from existing anticancer compounds within the GDSC and CCLE databases. Neighborhood was computed using Tanimoto similarity,  $\tau$ .

The third closest neighbor of the generated compound against neuroblastoma (Figure 5 first row, third column) is Fulvestrant. Interestingly, Fulvestrant is an antagonist/modulator of ER $\alpha$  (Estrogen receptor alpha) and has recently been proposed as a novel anticancer agent for neuroblastoma (Gorska et al. 2016).

The candidate compound proposed against breast cancer (Figure 5 second row, third column), has as a nearest neighbor Doxorubicin ( $\tau = 0.25$ ). Doxorubicin is a commonly used chemotherapeutic against breast cancer (Lao et al. 2013).

The generated compound against lung cancer (Figure 5, third row, third column) results close to Embelin, an existing anticancer compound from the GDSC database. Comparing the two structures, it is evident that the generated compound and Embelin share a long carbon chain and a single six-membered fully carbonic ring. In addition, Embelin was tested against 965 cell lines from GDSC/CCLE from which the highest reported efficacy is against a lung cell line (NT2-D1). Quantitatively speaking, the two molecules have a dice similarity (Dice 1945) of  $S_D = 0.39$  of ECFPs with radius 2 and a Tanimoto similarity of  $\tau = 0.24$ . Embelin is indeed known to be a promising anticancer compound as it is the only known non-peptide inhibitor of the XIAP protein (Poojari 2014). XIAP plays an important role in lung cancer development via its anti-apoptotic properties by which it protects lung tumors from chemotherapeutic drugs such as Cisplatin (Cheng et al. 2010).

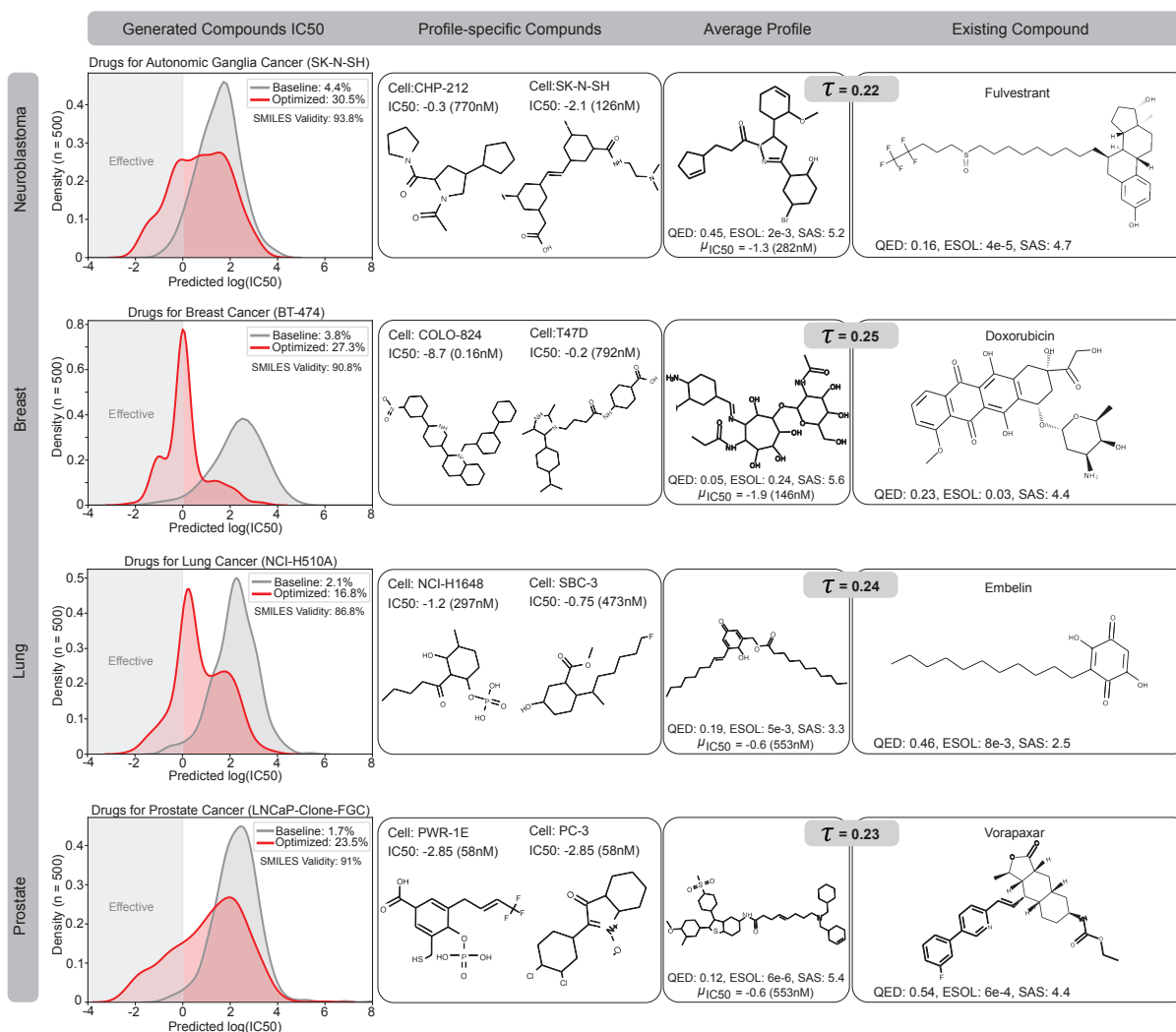


**Figure 5: Sample results for profile-driven model optimization and anticancer compound generation.** Each row illustrates the results of training the RL pipeline on cell lines from a specific site, namely neuroblastoma (autonomic ganglia), breast, lung and prostate cancer. The first column compares the distributions of IC<sub>50</sub> predictions given by the critic model for a set of  $n=500$  molecular structures generated with RL optimization (in red) and without RL optimization (in grey). As demonstrated by the density plots, the optimized candidate compounds have a lower mean IC<sub>50</sub> for the target cancer, highlighting the successful optimization of the generative model towards the design of more effective compounds. The second column presents candidate compounds with a high efficacy against a particular cell line that was not seen during training. The associated IC<sub>50</sub> drug sensitivity for the cell-compound pair is shown for each compound. The third column showcases generated compounds that were optimized to be effective against the average cell-line profiles of the given cancer type in each row. In the **fourth** column, we present an existing anticancer compound, from GDSC and CCLE databases, that was in the top-3 neighborhood (metric: Tanimoto similarity) of the generated compound in the third column. The existing and generated compounds are compared in terms of Tanimoto structural similarity as well as three chemical scores crucial in drug design namely, druglikeness (QED, 0 worst, 1 best), synthesizability (SAS, 1 best, 10 worst) and solubility (ESOL, given in  $M/L$ ).

Lastly, the closest neighbor ( $\tau = 0.23$ ) of the prostate-specific generated compound (Figure 5 fourth row, third column) is Vorapaxar, with its efficacy being highest against a prostate cancer cell line (DU\_145) according to GDSC/CCLE. Vorapaxar is an antagonist of a protease-activated receptor (PAR-1) that is known to be overexpressed in various types of cancer, including prostate (Zhang et al. 2009).

It should be noted that whether or not a candidate compound is considered promising, does not depend only on the predicted efficacy. There are other crucial properties with high relevance in drug design, such as cytotoxicity, druglikeness, synthesizability or solubility which are all quantifiable from the raw SMILES string of a compound. While we do believe the results of Figure 5 to be promising, there remains



further optimization of the model to be done as the future direction of our work. For instance, our conditional generator was not explicitly optimized for druglikeness, synthesizability and solubility. Within our RL optimization framework, further critics can be added that reward or punish the conditional generator for these other critical properties, in addition to efficacy against a given cancer profile.

## Discussion

We herein presented the first deep-learning based anti-cancer compound generator that enables us to condition the molecular generation on the biomolecular profile (transcriptomic profile in this work) of the target cell, tumor or cancer site. We demonstrated, using a reinforcement learning optimization framework, that our proposed generative model could be optimized to produce candidate compounds with high predicted efficacy (IC<sub>50</sub>) against a given target profile. We harnessed this capability to generate four candidate compounds against 4 common cancer types: neuroblastoma, lung, breast and prostate. We demonstrated in a post-hoc analysis that each of the four site-specific generated compounds had structural similarities to known anticancer compounds commonly used to treat cancer of the same type as the generated compound was optimized for. While we believe our results to be a promising stepping stone for profile-specific anticancer compound generation, we are aware further optimization must be done before it can be used a reliable tool for drug discovery. For instance, there are various other properties of a candidate drug other than its efficacy that determine its potential for becoming a successful anticancer compound. For future direction of this work, we aim to design the reward function in such a way that it computes rewards not only for efficacy but also for cytotoxicity, solubility, drug-likeness, molecular weight and synthesizability.

## References

- [Arun 2009] Arun, B. 2009. Challenges in drug discovery: Can we improve drug development. *Journal of Bioanalysis & Biomedicine* 1(1):1–4.
- [Barretina et al. 2012] Barretina, J.; Caponigro, G.; Stransky, N.; Venkatesan, K.; Margolin, A. A.; Kim, S.; Wilson, C. J.; Lehár, J.; Kryukov, G. V.; Sonkin, D.; et al. 2012. The cancer cell line encyclopedia enables predictive modelling of anticancer drug sensitivity. *Nature* 483(7391):603.
- [Bento et al. 2013] Bento, A. P.; Gaulton, A.; Hersey, A.; Bellis, L. J.; Chambers, J.; Davies, M.; Krüger, F. A.; Light, Y.; Mak, L.; McGlinchey, S.; Nowotka, M.; Papadatos, G.; Santos, R.; and Overington, J. P. 2013. The ChEMBL bioactivity database: an update. *Nucleic Acids Research* 42(D1):D1083–D1090.
- [Bickerton et al. 2012] Bickerton, G. R.; Paolini, G. V.; Besnard, J.; Muresan, S.; and Hopkins, A. L. 2012. Quantifying the chemical beauty of drugs. *Nature chemistry* 4(2):90.
- [Bjerrum and Sattarov 2018] Bjerrum, E., and Sattarov, B. 2018. Improving chemical autoencoder latent space and molecular de novo generation diversity with heteroencoders. *Biomolecules* 8(4):131.
- [Bowman et al. 2015] Bowman, S. R.; Vilnis, L.; Vinyals, O.; Dai, A. M.; Jozefowicz, R.; and Bengio, S. 2015. Generating sentences from a continuous space. *arXiv preprint arXiv:1511.06349*.
- [Brown et al. 2018] Brown, N.; Fiscato, M.; Segler, M. H.; and Vaucher, A. C. 2018. Guacamol: Benchmarking models for de novo molecular design. *arXiv preprint arXiv:1811.09621*.
- [Chen et al. 2018] Chen, H.; Engkvist, O.; Wang, Y.; Olivecrona, M.; and Blaschke, T. 2018. The rise of deep learning in drug discovery. *Drug discovery today*.
- [Cheng et al. 2010] Cheng, Y.-J.; Jiang, H.-S.; Hsu, S.-L.; Lin, L.-C.; Wu, C.-L.; Ghanta, V. K.; and Hsueh, C.-M. 2010. Xiap-mediated protection of h460 lung cancer cells against cisplatin. *European journal of pharmacology* 627(1-3):75–84.
- [Chomsky 1956] Chomsky, N. 1956. Three models for the description of language. *IRE Transactions on information theory* 2(3):113–124.
- [Dice 1945] Dice, L. R. 1945. Measures of the amount of ecologic association between species. *Ecology* 26(3):297–302.
- [Ertl and Schuffenhauer 2009] Ertl, P., and Schuffenhauer, A. 2009. Estimation of synthetic accessibility score of drug-like molecules based on molecular complexity and fragment contributions. *Journal of cheminformatics* 1(1):8.
- [Gaulton et al. 2016] Gaulton, A.; Hersey, A.; Nowotka, M.; Bento, A. P.; Chambers, J.; Mendez, D.; Mutowo, P.; Atkinson, F.; Bellis, L. J.; Cibrián-Uhalte, E.; et al. 2016. The ChEMBL database in 2017. *Nucleic acids research* 45(D1):D945–D954.
- [Gomez-Bombarelli et al. 2018] Gomez-Bombarelli, R.; Wei, J. N.; Duvenaud, D.; Hernandez-Lobato, J. M.; Sanchez-Lengeling, B.; Sheberla, D.; Aguilera-Iparraguirre, J.; Hirzel, T. D.; Adams, R. P.; and Aspuru-Guzik, A. 2018. Automatic chemical design using a data-driven continuous representation of molecules. *ACS central science* 4(2):268–276.
- [Goodfellow et al. 2014] Goodfellow, I.; Pouget-Abadie, J.; Mirza, M.; Xu, B.; Warde-Farley, D.; Ozair, S.; Courville, A.; and Bengio, Y. 2014. Generative adversarial nets. In *Advances in neural information processing systems*, 2672–2680.
- [Gorska et al. 2016] Gorska, M.; Kuban-Jankowska, A.; Milczarek, R.; and Wozniak, M. 2016. Nitro-oxidative stress is involved in anticancer activity of 17 $\beta$ -estradiol derivative in neuroblastoma cells. *Anticancer research* 36:1693–8.
- [Hopcroft and Ullman 1969] Hopcroft, J. E., and Ullman, J. D. 1969. *Formal Languages and Their Relation to Automata*. Boston, MA, USA: Addison-Wesley Longman Publishing Co., Inc.
- [Joulin and Mikolov 2015] Joulin, A., and Mikolov, T. 2015. Inferring algorithmic patterns with stack-augmented recurrent nets. In *Advances in neural information processing systems*, 190–198.
- [Kang and Cho 2018] Kang, S., and Cho, K. 2018. Condi-

- tional molecular design with deep generative models. *Journal of chemical information and modeling*.
- [Kingma and Ba 2014] Kingma, D. P., and Ba, J. 2014. Adam: A method for stochastic optimization. *arXiv preprint arXiv:1412.6980*.
- [Kingma and Welling 2013] Kingma, D. P., and Welling, M. 2013. Auto-encoding variational bayes. *arXiv preprint arXiv:1312.6114*.
- [Lao et al. 2013] Lao, J.; Madani, J.; Puértolas, T.; Álvarez, M.; Hernández, A.; Pazo-Cid, R.; Artal, Á.; and Antón Torres, A. 2013. Liposomal doxorubicin in the treatment of breast cancer patients: a review. *Journal of drug delivery* 2013.
- [Makhzani et al. 2015] Makhzani, A.; Shlens, J.; Jaitly, N.; Goodfellow, I.; and Frey, B. 2015. Adversarial autoencoders. *arXiv preprint arXiv:1511.05644*.
- [Manica et al. 2019] Manica, M.; Oskooei, A.; Born, J.; Subramanian, V.; Sáez-Rodríguez, J.; and Martínez, M. R. 2019. Towards explainable anticancer compound sensitivity prediction via multimodal attention-based convolutional encoders. *arXiv preprint arXiv:1904.11223 (presented at ICML 2019 workshop: "Workshop on Computational Biology")*.
- [Menden 2016] Menden, M. P. 2016. *In silico models of drug response in cancer cell lines based on various molecular descriptors*. Ph.D. Dissertation, University of Cambridge.
- [Oskooei et al. 2018a] Oskooei, A.; Born, J.; Manica, M.; Subramanian, V.; Sáez-Rodríguez, J.; and Martínez, M. R. 2018a. Pacmann: Prediction of anticancer compound sensitivity with multi-modal attention-based neural networks. *arXiv preprint arXiv:1811.06802 (presented at NeurIPS 2018 workshop: "Workshop for Machine Learning for Molecules and Materials")*.
- [Oskooei et al. 2018b] Oskooei, A.; Manica, M.; Mathis, R.; and Martínez, M. R. 2018b. Network-based biased tree ensembles (NetBiTE) for drug sensitivity prediction and drug sensitivity biomarker identification in cancer. *arXiv preprint arXiv:1808.06603 (presented at ICML 2019 workshop: "Workshop on Computational Biology")*.
- [Pagnoni, Liu, and Li 2018] Pagnoni, A.; Liu, K.; and Li, S. 2018. Conditional variational autoencoder for neural machine translation. *arXiv preprint arXiv:1812.04405*.
- [Polishchuk, Madzhidov, and Varnek 2013] Polishchuk, P. G.; Madzhidov, T. I.; and Varnek, A. 2013. Estimation of the size of drug-like chemical space based on gdb-17 data. *Journal of computer-aided molecular design* 27(8):675–679.
- [Poojari 2014] Poojari, R. 2014. Embelin—a drug of antiquity: shifting the paradigm towards modern medicine. *Expert opinion on investigational drugs* 23(3):427–444.
- [Popova, Isayev, and Tropsha 2018] Popova, M.; Isayev, O.; and Tropsha, A. 2018. Deep reinforcement learning for de novo drug design. *Science advances* 4(7):eaap7885.
- [Rosca et al. 2017] Rosca, M.; Lakshminarayanan, B.; Warde-Farley, D.; and Mohamed, S. 2017. Variational approaches for auto-encoding generative adversarial networks. *arXiv preprint arXiv:1706.04987*.
- [Said Fatahala et al. 2015] Said Fatahala, S.; Ahmed Shalaby, E.; Emam Kassab, S.; and Said Mohamed, M. 2015. A promising anti-cancer and anti-oxidant agents based on the pyrrole and fused pyrrole: synthesis, docking studies and biological evaluation. *Anti-Cancer Agents in Medicinal Chemistry (Formerly Current Medicinal Chemistry-Anti-Cancer Agents)* 15(4):517–526.
- [Savjani, Gajjar, and Savjani 2012] Savjani, K. T.; Gajjar, A. K.; and Savjani, J. K. 2012. Drug solubility: importance and enhancement techniques. *ISRN pharmaceuticals* 2012.
- [Scannell et al. 2012] Scannell, J. W.; Blanckley, A.; Boldon, H.; and Warrington, B. 2012. Diagnosing the decline in pharmaceutical r&d efficiency. *Nature reviews Drug discovery* 11(3):191.
- [Schneider 2019] Schneider, G. 2019. Mind and machine in drug design. *Nature Machine Intelligence* 1.
- [Sohn, Lee, and Yan 2015] Sohn, K.; Lee, H.; and Yan, X. 2015. Learning structured output representation using deep conditional generative models. In *Advances in neural information processing systems*, 3483–3491.
- [Szklarczyk et al. 2014] Szklarczyk, D.; Franceschini, A.; Wyder, S.; Forslund, K.; Heller, D.; Huerta-Cepas, J.; Simonovic, M.; Roth, A.; Santos, A.; Tsafou, K. P.; et al. 2014. String v10: protein–protein interaction networks, integrated over the tree of life. *Nucleic acids research* 43(D1):D447–D452.
- [Vaswani et al. 2017] Vaswani, A.; Shazeer, N.; Parmar, N.; Uszkoreit, J.; Jones, L.; Gomez, A. N.; Kaiser, Ł.; and Polosukhin, I. 2017. Attention is all you need. In *Advances in Neural Information Processing Systems*, 5998–6008.
- [Wang, Schwing, and Lazechnik 2017] Wang, L.; Schwing, A.; and Lazechnik, S. 2017. Diverse and accurate image description using a variational auto-encoder with an additive gaussian encoding space. In *Advances in Neural Information Processing Systems*, 5756–5766.
- [Weinstein et al. 2013] Weinstein, J. N.; Collisson, E. A.; Mills, G. B.; Shaw, K. R. M.; Ozenberger, B. A.; Ellrott, K.; Shmulevich, I.; Sander, C.; Stuart, J. M.; Network, C. G. A. R.; et al. 2013. The cancer genome atlas pan-cancer analysis project. *Nature genetics* 45(10):1113.
- [Williams and Zipser 1989] Williams, R. J., and Zipser, D. 1989. A learning algorithm for continually running fully recurrent neural networks. *Neural computation* 1(2):270–280.
- [Williams 1992] Williams, R. J. 1992. Simple statistical gradient-following algorithms for connectionist reinforcement learning. *Machine learning* 8(3-4):229–256.
- [Yang et al. 2012] Yang, W.; Soares, J.; Greninger, P.; Edelman, E. J.; Lightfoot, H.; Forbes, S.; Bindal, N.; Beare, D.; Smith, J. A.; Thompson, I. R.; et al. 2012. Genomics of drug sensitivity in cancer (gdsc): a resource for therapeutic biomarker discovery in cancer cells. *Nucleic acids research* 41(D1):D955–D961.
- [Yang et al. 2018] Yang, H.; Sun, L.; Li, W.; Liu, G.; and Tang, Y. 2018. In silico prediction of chemical toxicity for drug design using machine learning methods and structural alerts. *Frontiers in chemistry* 6:30.

[Zhang et al. 2009] Zhang, X.; Wang, W.; True, L. D.; Vessella, R. L.; and Takayama, T. K. 2009. Protease-activated receptor-1 is upregulated in reactive stroma of primary prostate cancer and bone metastasis. *The Prostate* 69(7):727–736.